SLOPE-DEPENDENT BIOPHYSICAL MODELING OF SURF ZONE LARVAL TRANSPORT

Atsushi Fujimura[1], Ad Reniers[1], Claire Paris[1], Alan Shanks[2], Jamie MacMahan[3], and Steven Morgan[4]

Abstract

Onshore transport of intertidal invertebrate larvae at a reflective (steep beach slope) and an intermediate (relatively gradual beach slope) beach is modeled. Physical model calculations are conducted with the measured bathymetry data and averaged wave data obtained during the summer of 2010 at Sand City beach, CA (intermediate beach) and the summer of 2011 at Carmel River State Beach, CA (reflective beach). The physical model output is then used in a Lagrangian larval tracking model. Our results show that larval delivery to the surf zone is higher at the more dissipative beach than at the more reflective beach, and this is consistent with the larval recruitment study by Shanks et al. (2010). Also, two possible factors for the successful onshore larval transport on an intermediate beach, turbulent-dependent sinking behavior and buoyancy of larvae, are not always necessary in the case of a reflective beach.

Key words: bio-physical interaction, modeling, surf zone, larval transport, beach morphology

1. Introduction

Most invertebrate larvae are slow swimmers that depend on water currents and other physical forcing to migrate onshore for settlement. Biological factors such as larval buoyancy and a sinking rate can also be of importance. The surf zone is the last stage in the migration of the larvae of intertidal invertebrate; however, the mechanism of larval delivery across this very energetic region is not well understood.

Shanks et al. (2010) showed that a larval settlement rate is higher at dissipative beaches (gradual beach slope) than reflective beaches (steep beach slope). Here we examine the effects of physical, biological, and morphological factors on larval transport at reflective and intermediate (between dissipative and reflective) beaches by using biophysical numerical modeling to help explain these observations.

2. Methods

2.1. *Field data*

Physical data were collected at Sand City beach, Monterey Bay, CA in the summer of 2010, and at Carmel River State Beach (CRSB), CA in the summer of 2011 (Figure 1). Sand City beach is characterized as an intermediate beach, and well-formed rip channels and shoals can be observed. CRSB is a reflective beach with a very narrow surf zone of $O(10)$ m. Current and wave data were obtained by releasing and monitoring drifters and dye, as well as fixed instruments such as acoustic Doppler current profilers. Bathymetric data used for the model simulations were collected with a personal water craft or kayak equipped with an echo sounder and a Global Positioning System (GPS). The dry beach and inter-tidal area where mapped by a walking person carrying a GPS backpack.

[1]RSMAS, University of Miami, 4600 Rickenbacker Causeway, Miami, FL 33149, USA. afujimura@rsmas.miami.edu, areniers@rsmas.miami.edu, cparis@rsmas.miami.edu
[2]OIMB, University of Oregon, 63466 Boat Basin Road, Charleston, OR 97420, USA. ashanks@uoregon.edu
[3]Naval Postgraduate School, 1 University Way Monterey, CA 93943, USA. jhmacmah@nps.edu
[4]BML, University of California, Davis, 2099 Westside Road, Bodega Bay, CA 94923, USA. sgmorgan@ucdavis.edu

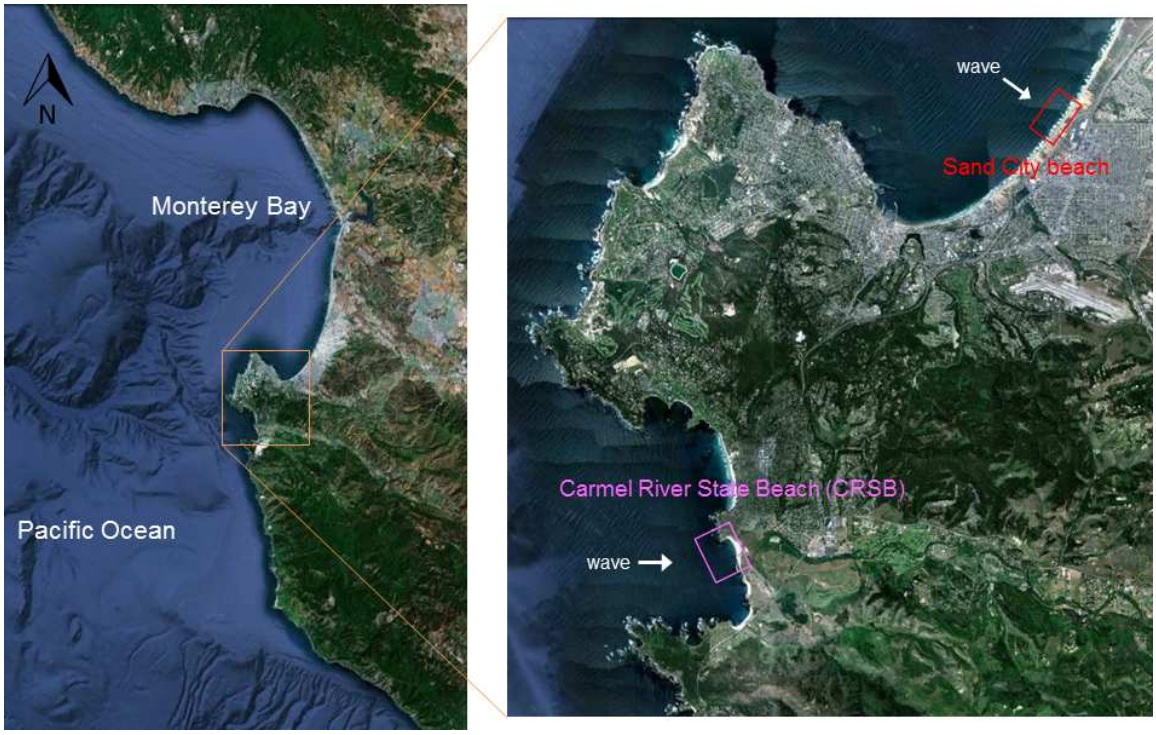

Figure 1. The locations of Sand City beach and Carmel River State Beach (CRSB) with the approximate model domains enclosed by red and pink rectangles, respectively (Credit: Google Earth). The average wave directions during the field experiment are indicated with arrows.

2.2. *Model setting*

2.2.1. *Hydrodynamic model*

For the three-dimentional hydrodynamic model simulations of both surf zones, we use the Computational Fluid Dynamics (CFD) software Delft3D (Deltares 2011a,b) including wave-current interaction.

For Sand City, the model domain consists of 850 m in the alongshore direction, 450 m in cross-shore direction, and depth is based on the collected bathymetry data. The model mesh scheme is a regular grid (hexahedral cells). Grid spacing is 10 m along the beach, approximately 5–10 m in the cross-shore with the finest at the shoreline, and 14 σ-layers representing the depth with a fine mesh near the bed in order to resolve bottom boundary layer streaming. Shoreline reflections are absorbed by an offshore Riemann boundary which is a weakly reflective open boundary. Onshore and alongshore boundaries are closed. A k-ε closure scheme is used for modeling turbulence by solving turbulent kinetic energy (k) and energy dissipation rate (ε). Shore normal waves with 0.75 m significant wave height and 8.75 s peak wave period, based on the average wave data during the data collection period in the summer of 2010, are generated at the offshore boundary. We also test effects of wind stress by imposing either no wind or 8.0 m s^{-1} constant onshore wind based on the approximate minimum and maximum values during the field experiment.

In the model settings for CRSB, we use the domain size of 1050 m alongshore and 600 m in the cross-shore. Cross-shore reflections are again managed by an offshore Riemann boundary, and alongshore reflections are suppressed by a weakly reflective water level boundary in the South, while the North side is a closed boundary. In the analysis we removed of the 50 m of the northern and 100 m of the southern end in order to eliminate potentially adversely affected boundary currents. Oblique waves with 0.57 m significant wave height and 9.45 s peak wave period, based on the average wave data during the experiment period in the summer of 2011, are generated at the offshore boundary. Due to shoaling from deeper water at CRSB the wave height at wave breaking is similar to the wave breaking height at Sand City beach. The other settings are the same as those used for the modeling at Sand City beach.

Model domains and depth contours with approximate surf zone edges are shown in Figure 2. Note that North points toward the bottom (offshore to the right) due to our coordinate system.

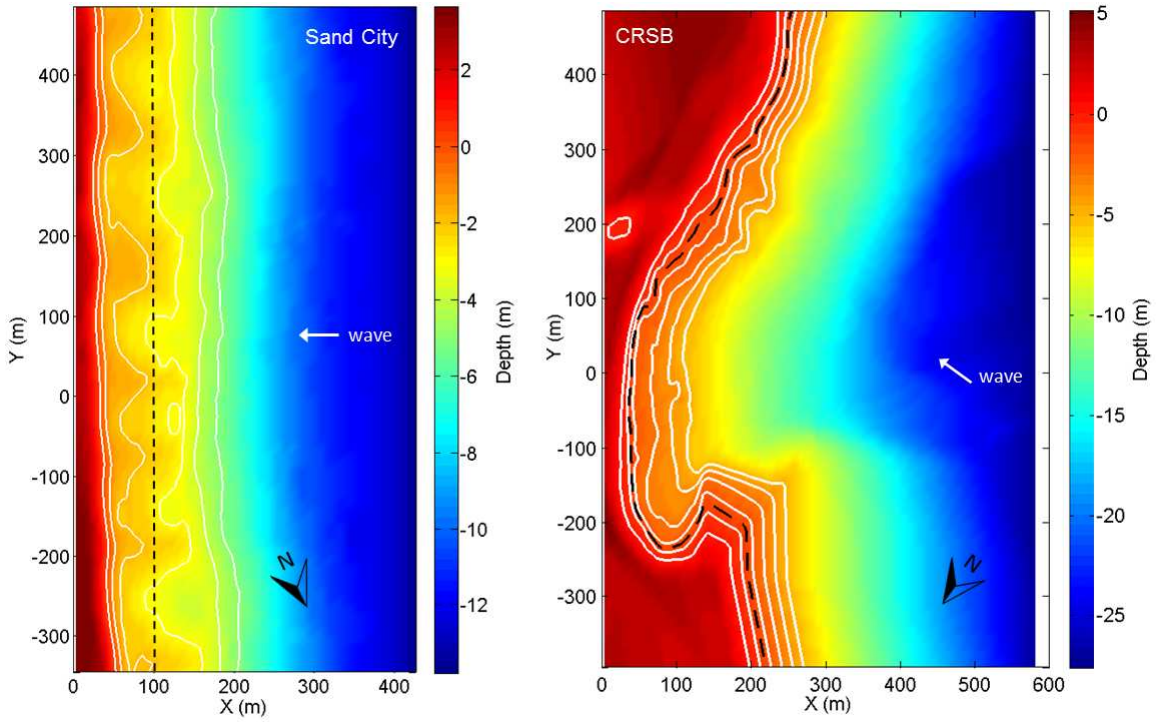

Figure 2. Bathymety in Sand City (left) and CRSB (right). White bottom contour lines are in 1 m increments from depth of 0 m (shoreline) to 5 m. Black dashed lines are the approximate surf zone edges as a reference. North direction is shown. The modeled wave angles obtained from time-averaged field data are indicated by white arrows.

Beach profiles consist of 1/7 subaerial beach slope, 1/89 subaqueous beach step, and 1/27 subaqueous beach profile along the rip channel (Y = 90 m) in Sand City; 1/8 subaerial beach slope, 1/64 subaqueous beach step, and 1/27 subaqueous beach profile along the shoal (Y = 160 m) in Sand City; and 1/6 subaerial beach slope, and 1/18 subaqueous beach profile at Y = 0 m in CRSB (Figure 3).

For both beaches, the model run time is 2 h with a time step size of 3 s and output interval is 6 s. Diurnal events, such as tide and diurnal wind cycle are not considered here, so the 2-h simulation output is used periodically for a 24-h larval transport simulation.

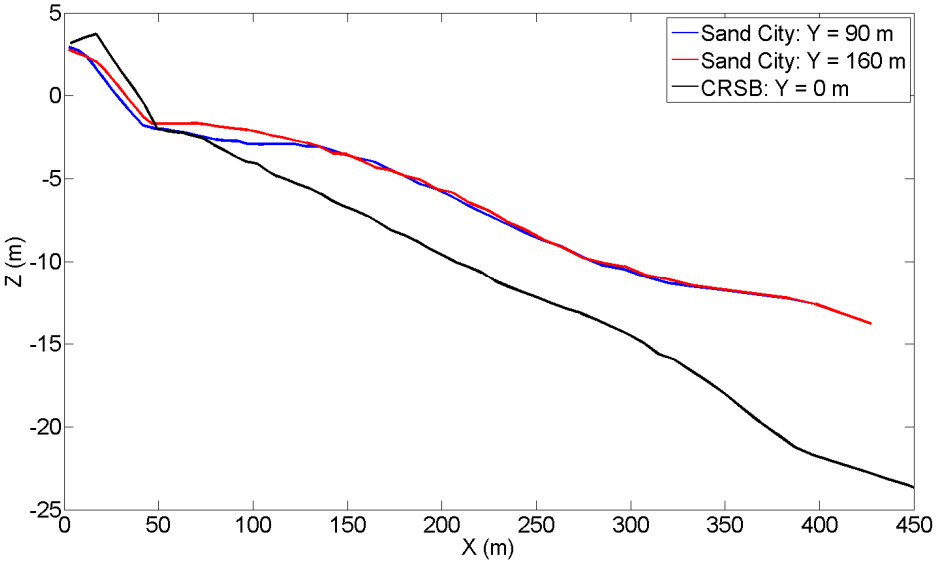

Figure 3. Beach profiles at Y = 90 m and 160 m for Sand City and at Y = 0 m for CRSB.

2.2.2. *Larval transport model*

An individual based model with the same Lagrangian transport equations as the ones used by Fujimura et al. (2013) is applied. For all the simulations presented here, Stokes drift is included, which plays a critical role in onshore larval transport (Fujimura et al., 2013). Another essential part of the transport mechanism is the turbulence-dependent sinking behavior (Fujimura et al. 2013) where competent larvae stop swimming and sink to the bottom by their own body weight when the turbulent energy dissipation rate is greater than 10^{-5} m^2 s^{-3} (Fuchs et al., 2004). Note that turbulent dissipation rates exceeding the threshold number occur almost everywhere in the bottom boundary layers and in the surf zones at both beaches.

Each individual particle is assigned a vertical velocity -10^{-3} m s^{-1} or $4*10^{-3}$ m s^{-1}, which represents buoyancy or vertical swimming speed of the larva. No active horizontal swimming behavior is considered here. In the 24-h simulation time, 602 particles for Sand City and 637 particles for CRSB are released every hour from offshore (X = 410 m for Sand City and X = 550 m for CRSB) equally distributed alongshore (Δy = 10 m) at two vertical locations for two types of particles: near the bottom for the particles with negative buoyancy (bottom dwellers); and near the water surface for the ones with positive buoyancy (surface migrators). For CRSB, we also released particles at X =350 m where the depth (10–15 m) is approximately the same as the offshore depth at Sand City (X = 410 m). Offshore and lateral sides are considered to be outlet boundaries, i.e., once a particle gets out of the model domain, it is not taken into account any more. The first 12-h run is used as a spin-up stage for particle initialization, and only second half of the simulation (12-24 h) is used to calculate the time-averaged particle density. The model cases and parameters are summarized in Table 1.

Table 1. Performed model cases. "Wind" is either no wind (no) or onshore wind (yes) = 8.0 m s^{-1}. "X" is initial cross-shore position of particles. "Sinking" is sinking behavior of particles, included (on) or not (off). "W" is vertical velocity of particles: negative (N) = -10^{-3} m s^{-1} or positive (P) = $4*10^{-3}$ m s^{-1}. Each case name describes a test condition: location and initial cross-shore particle positions are "i" = Sand City at 410 m, "ii" = CRSB at 550 m, and "iii" = CRSB at 350 m; "W" if onshore wind is included; "S" if the sinking behavior is included; "+" and "-" correspond to positive and negative buoyancy of particle, respectively. For example, Case 1.iS- is negatively buoyant particles with sinking behavior released at X = 410 m of Sand City beach during no wind event.

Case	Location	X (m)	Wind	Sinking	W
1.iS-	Sand City	410	no	on	N
2.iS+	Sand City	410	no	on	P
3.i-	Sand City	410	no	off	N
4.iWS-	Sand City	410	yes	on	N
5.iWS+	Sand City	410	yes	on	P
6.iW+	Sand City	410	yes	off	P
7.iiS-	CRSB	550	no	on	N
8.iiS+	CRSB	550	no	on	P
9.ii-	CRSB	550	no	off	N
10.iiiS-	CRSB	350	no	on	N
11.iiiS+	CRSB	350	no	on	P
12.iii-	CRSB	350	no	off	N
13.iiWS-	CRSB	550	yes	on	N
14.iiWS+	CRSB	550	yes	on	P
15.iiW+	CRSB	550	yes	off	P
16.iiiWS-	CRSB	350	yes	on	N
17.iiiWS+	CRSB	350	yes	on	P
18.iiiW+	CRSB	350	yes	off	P

3. Results and discussion

3.1. *Sand City beach*

Modeled time-averaged depth-integrated velocities at Sand City from the two physical model cases, without and with wind, are shown in Figure 4. In the surf zone, onshore currents enter over the shoals, then flow back offshore as rip currents. Wind stress change the current but the general flow patterns in the surf zone are similar to that in the no wind case.

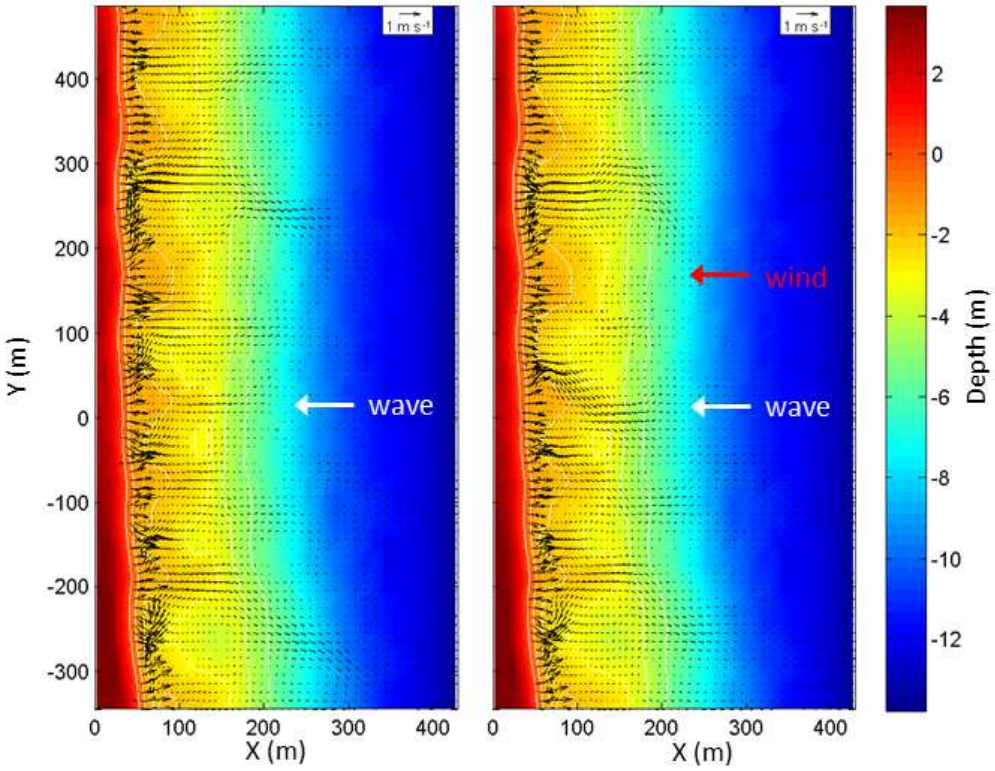

Figure 4. Time-averaged depth-integrated velocities with bathymetry at Sand City beach. No wind case (left) and onshore wind case (right). Arrows indicate the directions of wave and wind.

3.1.1. *No wind case*

Negatively buoyant particles with sinking behavior (Case 1.iS-) reached the surf zone, while the positively buoyant particles (Case 2.iS+) did not (Figure 5). Negatively buoyant particles without sinking behavior (Case 3.i-) partially entered the surf zone but not as significant as the particles with sinking behavior (Figure 5). Fujimura et al. (2013) explained a possible mechanism of the successful onshore larval migration that negatively buoyant larvae sink in the turbulent bottom boundary layer and are carried by streaming toward the shore. Note that the particle concentrations in Case 1.iS- were much higher in the rip than on the shoal (Figure 5) which was also shown by Fujimura et al. (2013).

3.1.2. *Onshore wind case*

In contrast to the no-wind case, negatively buoyant particles with sinking behavior (Case 4.iWS-) did not achieve onshore migration because wind forcing eventually altered the offshore current near the bed suppressing streaming (Figure 6). On the other hand, the positively buoyant particles (Case 5.iWS+) could reach the surf zone (Figure 6). The positively buoyant particles without sinking behavior (Case 6.iW+) partially entered the surf zone but mostly concentrated outside the surf zone (Figure 6). With onshore wind forcing, there is another possible mechanism of larval transport to the shore: positively buoyant larvae are carried by the wind driven onshore surface current, and they sink to the bottom in response to the turbulence once they get to the surf zone edge, and then they are caught by the bed streaming flowing toward the shore (Fujimura et al., 2013).

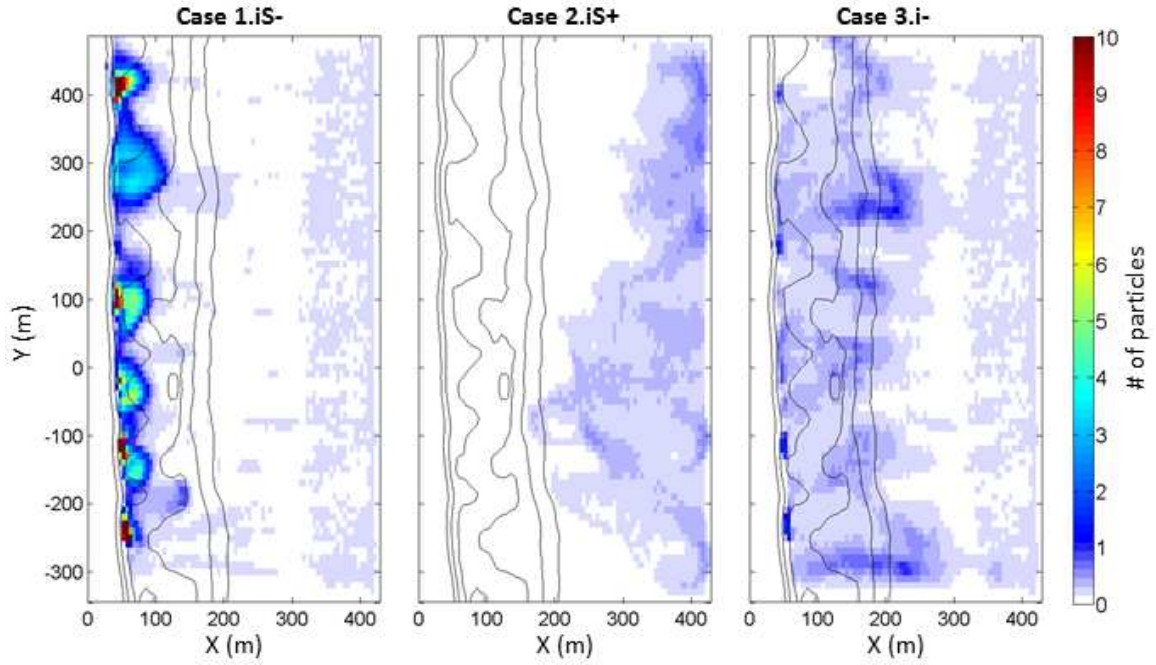

Figure 5. Depth- and time-averaged particle density (number of particles / unit volume) for the no wind case at Sand City beach. Left panel: Negatively buoyant particles with sinking behavior. Middle panel: Positively buoyant particles with sinking behavior. Right panel: Negatively buoyant particles without sinking behavior. Bottom contour lines from 0 m depth (shore line) to 5 m depth with 1 m increments are given.

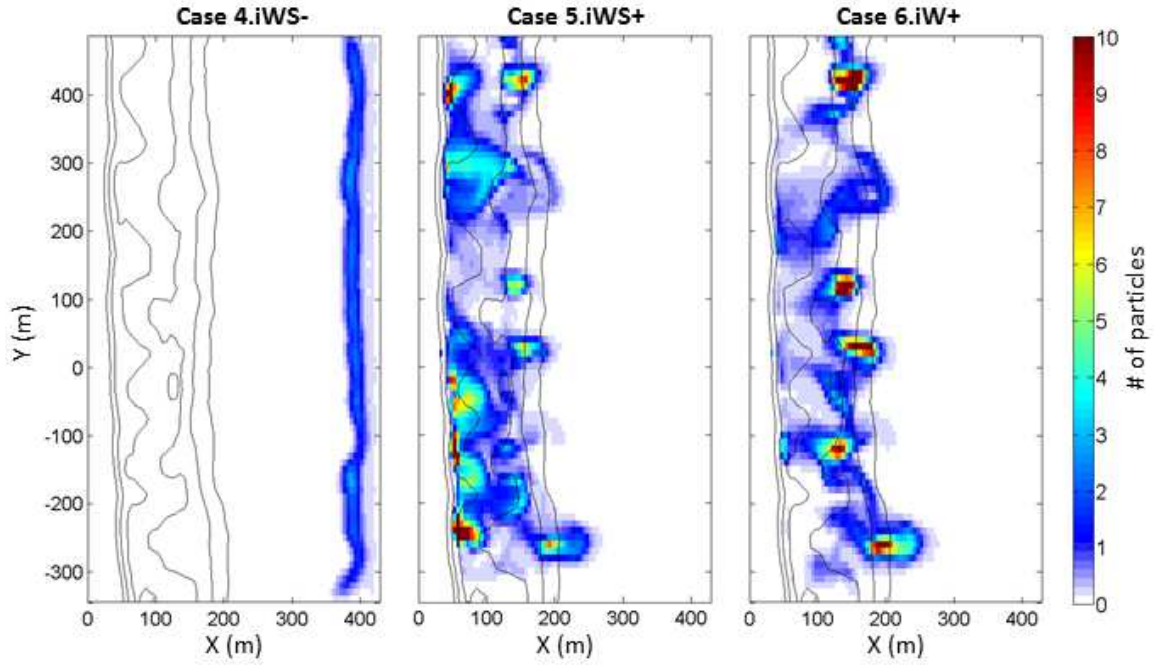

Figure 6. Depth- and time-averaged particle density (number of particles / unit volume) for the onshore wind case at Sand City beach. Left panel: Negatively buoyant particles with sinking behavior. Middle panel: P positively buoyant particles with sinking behavior. Right panel: Positively buoyant particles without sinking behavior. Bottom contour lines from 0 m depth (shore line) to 5 m depth with 1 m increments are given.

3.2. *Carmel River State Beach*

Time-averaged depth-integrated velocities at CRSB from the physical model output of with/without wind cases are shown in Figure 7. In both cases, flows entrained in the cove around X = 100 m × Y = -200 m, and continued as alongshore currents up to about Y = 200 m, where an eddy formed around X = 300 m. Wind forcing made the eddy somewhat larger and shifted it a little toward North.

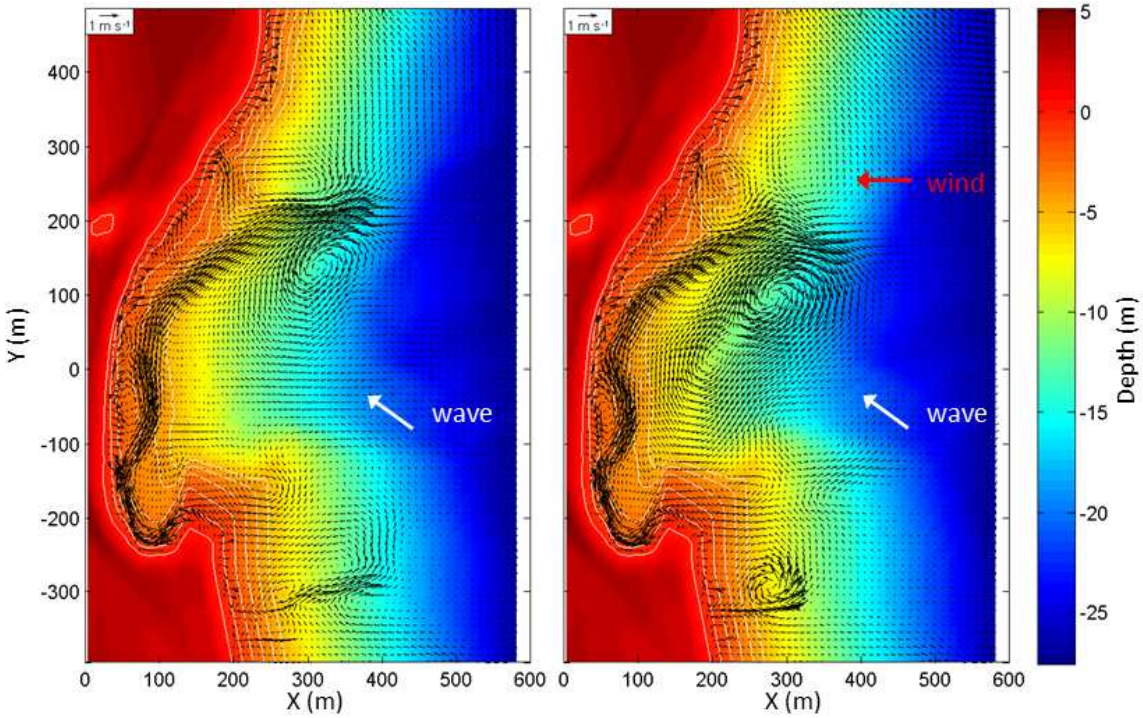

Figure 7. Time-averaged depth-integrated velocities with bathymetry at CRSB. No wind case (left) and onshore wind case (right). Arrows indicate the directions of wave and wind.

3.2.1. *No wind case*

Depth- and time-averaged particle concentrations for the no wind case at CRSB are shown in Figure 8. Negatively buoyant particles with sinking behavior released at X = 550 m (Case 7.iiS-) created some patches outside the surf zone but not in the surf zone. A very small number of particles got into the surf zone for positively buoyant particles with sinking behavior (Case 8.iiS+) and negatively buoyant particles without sinking behavior (Case 9.ii-). Some particles with negative and positive buoyancy with sinking behavior (Cases 10.iiiS- and 11.iiiS+, respectively) and with negative buoyancy without sinking behavior (Case 12.iii-) released at X = 350 m reached the surf zone, but these were very patchy distributions. These high density particle patches in the surf zone tended to be in the south rather than the northern surf zone. The difference of particle concentrations between two different initial release locations (X = 550 m and 350 m) indicates differences in cross-shore flow patterns between offshore and near the surf zone. This also suggests that the influx of particles from the lateral boundaries closer to shore, which are not considered here, will be important.

There seems a correlation between the current pattern (Figure 7) and the particle patch distributions (Figure 8). A notable feature is the circulation at X = 300 m × Y = 150 m, where each case has a relatively high concentration patch at that location. Another common high concentration spot is at X = 50 m × Y = -50 m which is between the shoreline and the alongshore current and again coincides with the presence of an eddy trapping the particles.

By comparing the successful cases when particles entered the surf zone, it is obvious that the onshore larval transport rate at CRSB (Case 10.iiiS- in Figure 8) was much lower than that at Sand City beach (Case 1.iS- in Figure 5). Note that the color scale in Figure 8 is 10 times smaller than in Figure 5 even though the same amount of particles per unit volume was released. This is consistent with the study by

Shanks et al. (2010) who showed larvae of some intertidal species are delivered in a higher rate at more dissipative than more reflective beaches. Also, since some particles in both Cases 11.iiiS+ and 12.iii- entered the surf zone, the effects of particle buoyancy and the sinking behavior for onshore larval transport at CRSB without wind forcing seem to be less significant than for the same condition at the intermediate beach at Sand City.

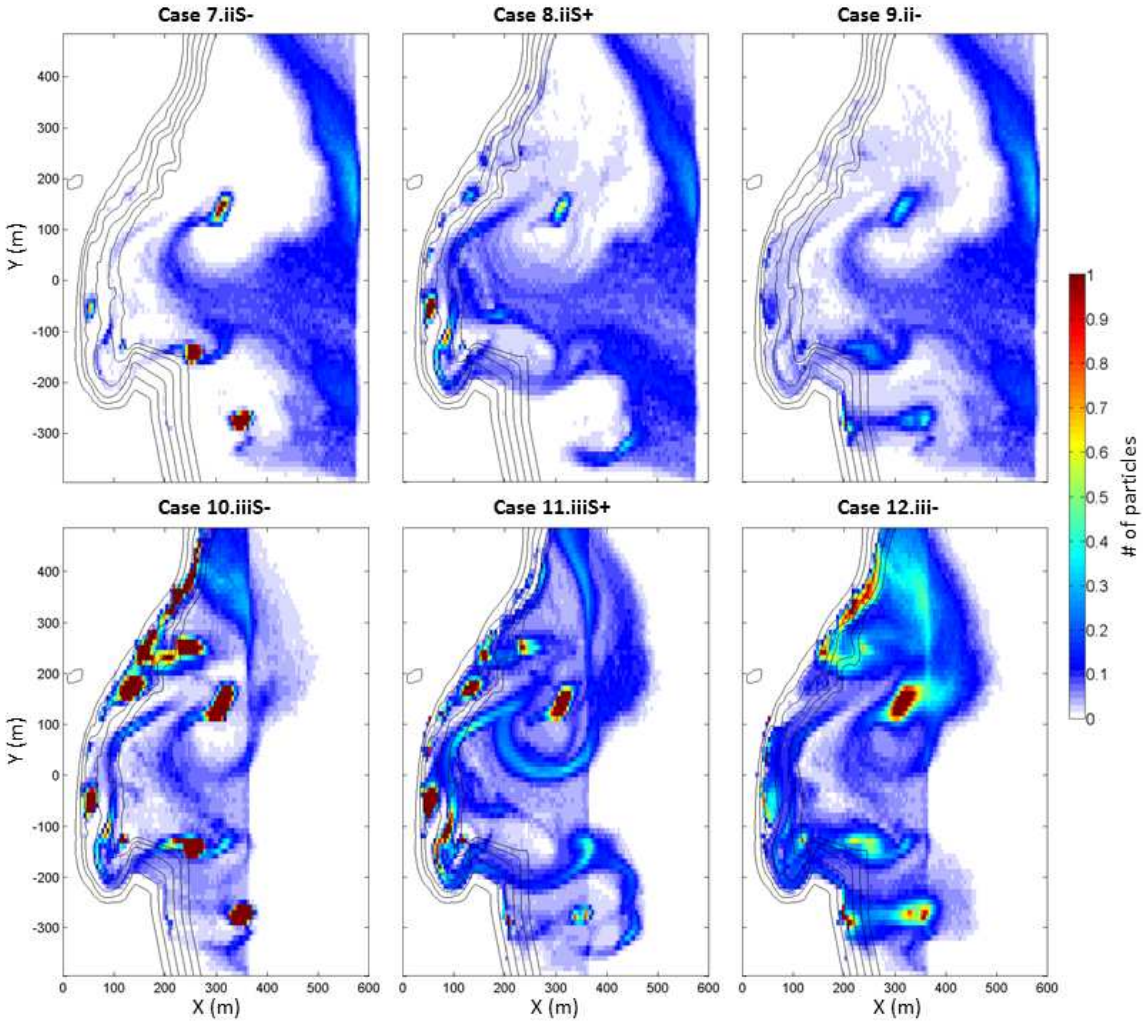

Figure 8. Depth- and time-averaged particle density (number of particles / unit volume) for the no wind case at CRSB. Initial cross-shore particle release positions are (upper panels) X = 550 m and (lower panels) X = 350 m. Left panels: Negatively buoyant particles with sinking behavior. Middle panels: Positively buoyant particles with sinking behavior. Right panels: Negatively buoyant particles without sinking behavior. Bottom contour lines from 0 m depth (shore line) to 5 m depth with 1 m increments are given as a reference.

3.2.2. *Onshore wind case*

Figure 9 shows the depth- and time-averaged particle densities for the onshore wind case at CRSB. Negatively buoyant particles with sinking behavior released either at X = 550 m (Case 13.iiWS-) or 350 m (Case 16.iiiWS-) did not achieve onshore transport into the surf zone because the bottom boundary layer streaming was suppressed by the onshore wind stress. A relatively large patch can commonly be observed at X = 200 m × Y = 200 m in cases with positively buoyant particles; with sinking behavior released at X = 550 m (Case 14.iiWS+) and X = 350 m (Case 17.iiiWS+), and without sinking behavior released at X = 550 m (Case 15.iiW+) and X = 350 m (Case 18.iiiW+). This patch is caused by the eddy at the same location (right panel in Figure 7). Similarly to the no wind case, particles in these cases tend to accumulate in the South.

Positively buoyant particles without sinking behavior for both initial release locations (Cases 15.iiW+ and 18.iiiW+) were delivered to the shore more abundantly than in the case with sinking behavior (Cases 14.iiWS+ and 17.iiiWS+) (Figure 9). This result is opposite to the Sand City case (Figure 6) where positively buoyant particles with sinking behavior (Case 5.iWS+) reached shore at a higher rate than the ones without sinking behavior (Case 6.iW+). Thus, the significance of the sinking behavior varies with beach morphology and corresponding water flow. Again, note that the color scale in Figure 9 is smaller than in Figure 6.

Similarly to the no-wind case, the rate of successfully transported larvae at CRSB (Cases 14.iiWS+ and 17.iiiWS+ for comparison, but also even Cases 15.iiW+ and 18.iiiW+ in Figure 8) was lower than that at Sand City beach (Case 5.iWS+ in Figure 6). This result also supports the previous finding that intertidal invertebrate larvae were delivered at a higher rate at more dissipative than more reflective beaches (Shanks et al., 2010).

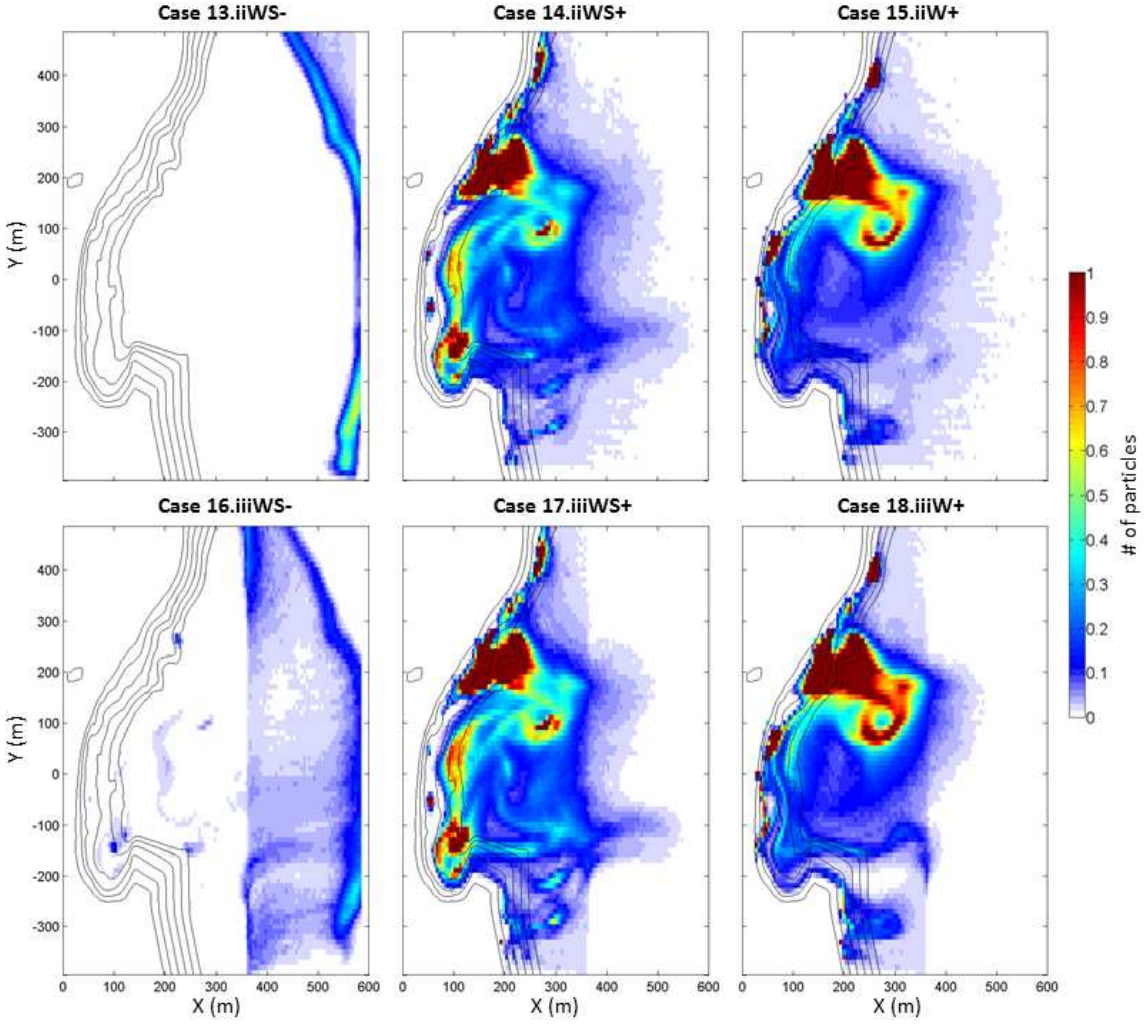

Figure 9. Depth- and time-averaged particle density (number of particles / unit volume) for the onshore wind case at CRSB. Initial cross-shore particle release positions are (upper panels) X = 550 m and (lower panels) X = 350 m. Left panel: Negatively buoyant particles with sinking behavior. Middle panels: Positively buoyant particles with sinking behavior. Right panels: Positively buoyant particles without sinking behavior. Bottom contour lines from 0 m depth (shore line) to 5 m depth with 1 m increments are given as a reference.

4. Conclusions

Our biophysical model showed the differences of larval transport on two types of beaches with various biological and physical parameters. The intermediate beach (Sand City) let the larvae cross the surf zone more easily than in the reflective beach (CRSB). This result supports the idea that larval delivery is higher at more dissipative beaches than at more reflective beaches (Shanks et al., 2010). There are two common cases where larvae achieve onshore transport in the both beaches: 1) negatively buoyant particles (bottom dwelling larvae) with turbulent-dependent sinking behavior in no wind condition; 2) positively buoyant particles (floating larvae) with turbulent sinking behavior during onshore wind event. Unlike Sand City beach, larvae could reach the surf zone without sinking behavior, especially for the positively buoyant particles with onshore wind forcing. Even positively buoyant larvae got into the surf zone during no-wind conditions. Therefore, larval transport at the relatively steep beach is less dependent on the important parameters for the gradual slope beach (i.e., larval buoyancy and the sinking behavior), but are more controlled by the more complex beach configuration and morphology.

Acknowledgements

This study is supported by National Science Foundation (OCE092735) “Collaborative Research: Does coupling between the inner shelf and surf zone regulate larval supply to intertidal populations?” We appreciate our colleagues, technicians, and students who helped with the field experiments. C. Paris is funded by National Science Foundation (OCE 1155698).

References

Deltares. 2011a. *Delft3D-FLOW User Manual, Version 3.15*, Delft,the Netherlands: Deltares.

Deltares. 2011b. *Delft3D-WAVE User Manual, Version 3.04*, Delft,the Netherlands: Deltares.

Fuchs, H. L., Mullineaux L. S. and Solow A. R., 2004. Sinking behavior of gastropod larvae (Ilyanassa obsoleta) in turbulence. *Limnology and Oceanography*, 49: 1937-1948.

Fujimura, A., Reniers A. J. H. M., Paris, C. B., Shanks, A. L., MacMahan, J. H., Morgan, S. G. 2013. Numerical simulations of larval transport into the surf zone. *Limnology and Oceanography*, submitted.

Shanks, A. L., Morgan, S. G., MacMahan, J. and Reniers, A. J. H. M., 2010. Surf zone physical and morphological regime as determinants of temporal and spatial variation in larval recruitment. *Journal of Experimental Marine Biology and Ecology*, 392: 140-150.